Sparkover Voltage Estimation of Standard Sphere Gaps for Negative Polarity by Calculation of Ionization Index

Yasuo Nishikori*, Soji Kojima* and Teruya Kouno*

Abstract - The field utilization factor η (the mean electric field / the maximum electric field) of standard sphere gaps was calculated by the charge simulation method, taking into account the ground plane and shanks. η changes mainly with g/r and slightly with l_1, l_2 and t, where D=2r is the sphere diameter, g is the gap length, l_1 and l_2, respectively, are the lengths of the upper and lower shank, and t is the shank diameter. Generally, η increases as l_1, l_2 and t each becomes larger. IEC standard 60052 (2002) limits $t \leq 0.2D$ $l_1 \geq 1D$ and prescribes $A=l_2+D+g$ where A is the height of the spark point on the upper sphere. Therefore, η is the largest when A=9D and the smallest when A=3D. The simple equation of a straight line, $\eta=1-(g/3r)$, can generally be used as a representative value of η for a wide variety of sphere diameters that are permitted by the IEC standard. The maximum electric field E_m at sparkover of standard air gaps has also been calculated by the relation $E_m=V/(\eta g)$. E_m describes a U-curve for g/r, up to the sphere diameter of 1 m. Moreover, for 1.5-m and 2-m diameters and especially for negative polarity, sparkover voltages have been calculated by integration of the ionization index.

Keywords: field utilization factor, maximum electric field at sparkover, Peek's equation, standard sphere gaps

1. Introduction

Although the corona threshold and spark breakdown voltages can be satisfactorily predetermined in cases where empirical formulas or curves are available, a more general applicable method is required.

The advent of the streamer theory and its later modifications led us to a general method of a breakdown criterion that is often adequate for accurate calculations but possibly lacking in rigor.

Pedersen [1] performed calculations of such a criterion for standard sphere gaps. The ionization index of these gaps was compared with those of the parallel plane electrode by using the same values of Sanders [2] for the field dependence of the ionization coefficient α in both electrode systems. The results were not entirely satisfactory because of inadequate knowledge of the axial field distributions in gap spacing.

Recent development in high-speed computer technology in connection with the study of high-voltage engineering has led to an increasing desire to evaluate the electrostatic field.

With respect to the electric field of a sphere gap, one of the authors has been researching the effects of the ground plane and shank on sparkover voltages using Pedersen's method (Nishikori et al. [3], [4]).

Interesting characteristics appeared when the field utilization factor for the calculated sphere gap and the maximum electric field at sparkover were considered. As a result, follow-up calculations were performed and are reported in this paper.

The axial field distributions in gap spacing up to the sphere radius, which covers all sizes of the standard diameters prescribed by IEC standard 60052 [5], are more exactly calculated by the charge simulation method, which takes into account the quantitative effects of both the ground plane and the shank geometry. Therefore, the field utilization factor η (the mean electric field / the maximum electric field) is also exactly calculated, depending on both the ground plane and the shank geometry.

Based on Pedersen's method and the exact results calculated by the charge simulation method, the sparkover voltages of standard sphere gaps for a wide variety of sphere diameters have been calculated especially for negative polarity.

The height A of the spark point on the upper sphere is prescribed by IEC standard 60052 as $A=l_2+D+g$ for individual sphere diameters D from 2 cm to 2 m.

Generally, the calculated sparkover voltage V_s changes

* Dept of Electrical Engineering, Kogakuin University, Shinjuku-ku, Tokyo, 163-8677, Japan (nisikori@cc.kogakuin.ac.jp)

Received November 4, 2003 ; Accepted January 19, 2004

mainly with the gap length g and slightly with the shank geometry, which consists of length l_1 of the upper shank, length l_2 of the lower shank and shank diameter t. V_s is related to the maximum field E_m at sparkover by the fundamental relation $E_m=V_s/(\eta g)$, which was developed by Schwaiger [6]. With respect to the longer gap length, the sparkover voltages could be closely matched by two empirical curves and a very sharp transition, which is known as the Toepler discontinuity [7]. An explanation by Meek [8] suggested that this discontinuity was caused by the breakdown mechanisms **1** and **2.**

In mechanism **1**, the avalanche must cross the whole gap length before breakdown. In mechanism **2**, the breakdown equation is fulfilled for a small fraction of the gap length, because α is virtually zero in the mid-gap region.

It is clear that the calculated results can provide a very detailed description, such as the Toepler discontinuity and the influences of the ground plane and the shank geometry on sparkover voltages.

2. Electric Field Calculation

The sparkover characteristics of the gas between two electrodes are closely related to the electric field distribution created by the applied voltage between the electrodes. In order to understand how individual influences of the ground plane and shank geometry contribute to the sparkover of the sphere gap, it is necessary to know how they affect the field distribution in the space between the spheres and particularly how they affect the regions of the sphere gaps which are the most stressed.

This paper describes a method which sets up the charge simulation method. This method deals with the field distribution along the central axis between the sphere electrodes in three dimensions with rotational symmetry.

In the charge simulation method, the potentials of fictitious charges of a point, line and ring, respectively, are taken as particular solutions of Laplace equation. These charges are placed outside the space in which the field is to be calculated, so that their integrated effect satisfies the boundary conditions exactly at a selected number of points on the boundary. Because the potentials due to these charges satisfy Laplace equation inside the space under consideration, the solution is unique inside that space.

2.1 Conditions for Calculation

Fig. 1 shows the arrangement for the electric field calculation performed by the charge simulation method. In this arrangement, when the ratios of the gap length g, the lengths of the upper shank l_1 and lower shank l_2 and the diameter of shank t (here, the diameters of both upper and lower shanks have the same value) with respect to the sphere diameter D are determined, the electric field is found to be essentially unique.

In the IEC standard, however, the ranges of height A of the spark points are prescribed, as shown in Table 1, and so there are some differences due to the sphere diameters.

Because of its discrete nature, the charge simulation method requires selection and displacement of a larger number of charges to achieve satisfactory accuracy.

Fig. 2 shows the arrangement of the contour points and fictitious charges in the upper electrode system.

In the region of the shank, there exist 11 line charges and 11 contour points corresponding to the line charges.

In the region of the sphere, there exist 1 point charge (the ring charge having a radius of zero), 36 ring charges, and 37 corresponding contour points.

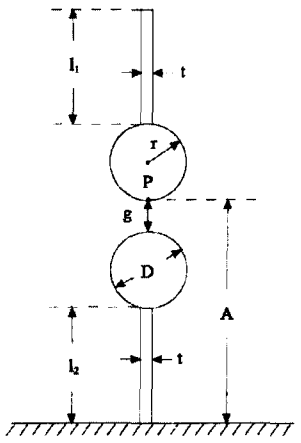

D=2r: Sphere diameter
g: Gap length
A: Height from the ground plane of point P where the field reaches a max
l_1: Length of the shank on the stress side
l_2: Length of the shank on the ground side
t: Diameter of the shanks

Fig. 1 Arrangement of vertical sphere gaps

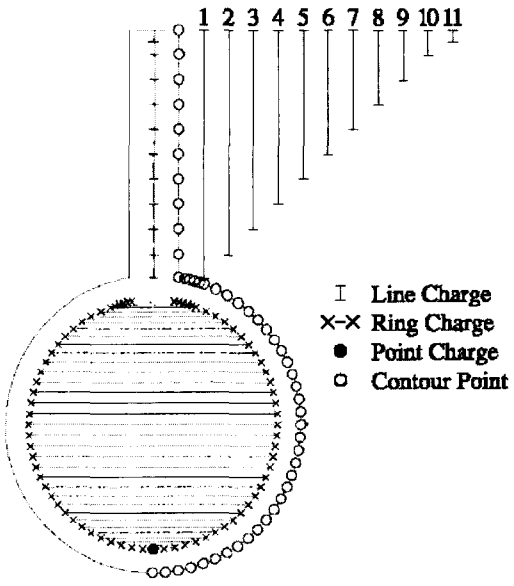

Fig. 2 Arrangement of fictitious charges and contour points

Table 1 Limits of height A by the IEC standard

D (cm)	Up to 6.25	10-15	25	50,75	100	150,200
Min of A	7D	6D	5D	4D	3.5D	3D
Max of A	9D	8D	7D	6D	5D	4D

In the lower electrode system, the arrangement is a mirror image of Fig. 2.

The total fictitious charges for all over the sphere gap electrode system are $2\times(37+11)=96$, and correspond to 96 contour points. Furthermore, the calculation taking into account the quantitative effect of the ground plane can be performed by including the image charges of all the fictitious charges.

2.2 Approximation of Field Utilization Factor

The field utilization factor η of standard sphere gaps was calculated by the charge simulation method, taking into account the ground plane and shanks, as shown in Fig. 1. η changes mainly by g/r and slightly by l_1, l_2 and t. Generally, η increases as l_1, l_2 and t each becomes larger. The IEC standard limits $t \leq 0.2D, l_1 \geq 1D$ and prescribes $A=l_2+D+g$, as shown in Table 1.

Therefore, η is the largest when A=9D and the smallest when A=3D, if the other values are constant. Fig. 3 shows the upper limit, lower limit and typical values of η.

Curve 3 in Fig. 3 is calculated using the lower limits of A and l_1, and an arbitrary lower limit for t. So, it is considered to be the lower limit of η. Curve 1 uses the upper limits of A and t, and an arbitrary upper limit for l_1. It is an example of the upper limit of η, because larger l_1 values up to infinity are permitted. Curve 2 is the straight line shown in (1) below.

$$\eta = 1-(g/3r) \tag{1}$$

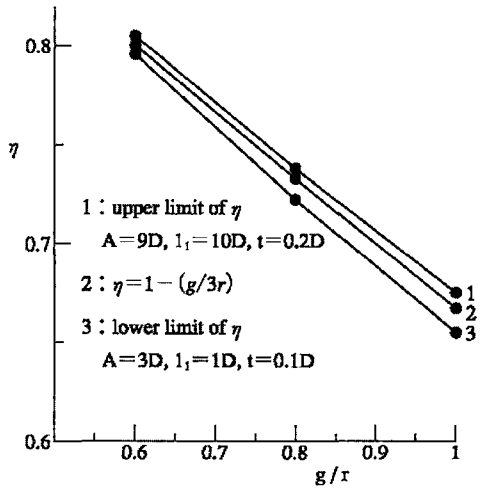

Fig. 3 Limits of field utilization factor η

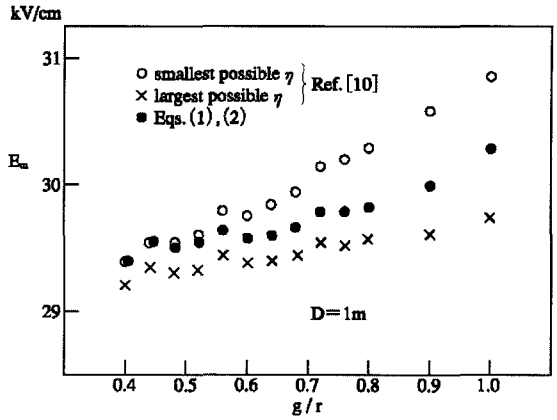

Fig. 4 Variations of the maximum electric field for the IEC standard clearance limit (D=1 m)

From Fig. 3, this simple equation can generally be used as a representative value of η, although the length and diameter of the shanks must change for the range permitted by the IEC standard.

We have also calculated the maximum electric field E_m at sparkover of standard air gaps, which is given by the following fundamental relation [6].

$$E_m = V/(\eta g) \tag{2}$$

where V is used for the standard value of sparkover listed in Table 2 of the IEC standard, and η is used for (1).

Peek's equation [9], given by (3) below, is often referred to as the maximum electric field at sparkover and it is that the right-hand side of the curve of Peek's equation, is almost constant, and dependent only on the sphere radius r.

$$E_m / p = 36.71\left(1+0.533/\sqrt{r}\right) \quad (V/cm/torr) \tag{3}$$

However, due to the effects of the ground plane that make η smaller and the effects of the upper shank that make η larger, part of the curve is expressed as monotonously increasing.

The curves of maximum electric field E_m, obtained from (1) and (2) describe a U-curve for g/r, up to the sphere diameter of 1 m. As shown in Fig. 4 for the sphere diameter of 1 m, the result obtained from (1) and (2), represented as (•), is compared with the results from the detailed analysis by Kowamoto et al. [10], represented as (○,×).

In Fig. 4, V is set at the standard values for IEC standard 60052, and the symbols (○) indicate the smallest possible η (l_1=1D, l_2=2D, t=0.05D) and the symbols (×) indicate the largest possible η ($l_1=\infty$, l_2=3.5D, t=0.2D).

Fig. 5 shows, that the curves of the maximum electric field for the 1.5- and 2-m diameter, in comparison with the

results obtained from the Peek's equation, are different from the U-form. The curve for the 1.5-m diameter has a maximum point at g=60 cm, and the curve for the 2-m has a maximum at 50 cm. The reason is that the standard values of IEC have irregularity at these points.

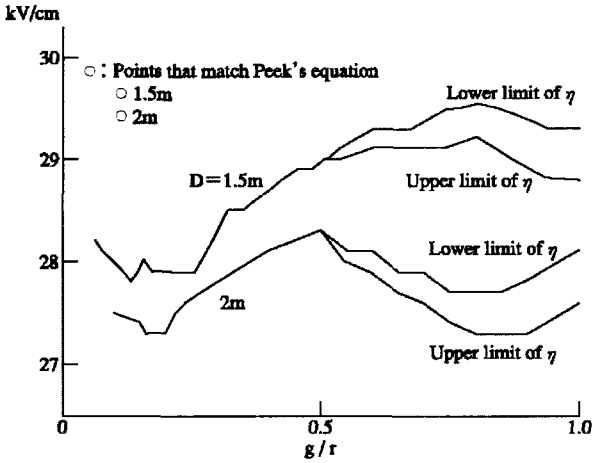

Fig. 5 Variations of the maximum electric field for the IEC standard clearance limit (D=1.5 m and 2 m)

3. Calculation of Sparkover Voltage

The sparkover voltage of standard sphere gaps was calculated by Pedersen's breakdown criterion [1], in which the criterion can be used to correlate the sparkover voltage in a uniform field with the sparkover voltage in a non-uniform field of known field distribution.

Therefore, integration of the ionization index along an axial non-uniform field in standard sphere gaps, calculated from the charge simulation method, is compared with the integration along a uniform field in parallel plate electrodes, evaluated by (4) below, using the same values for the ionization coefficient α for field dependence. Fig. 6 shows the field dependence of ionization coefficient α, referred to in [2].

$$E_m / p = 31.64\left(1+0.328/\sqrt{g}\right) \quad (V/cm/torr) \qquad (4)$$

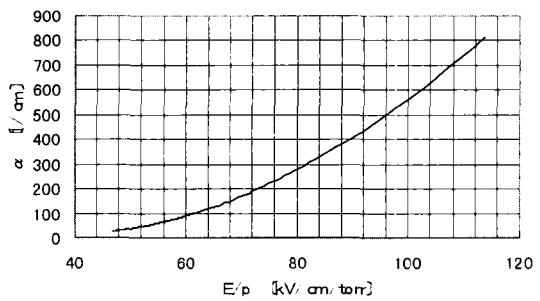

Fig. 6 Field dependence of ionization coefficient α

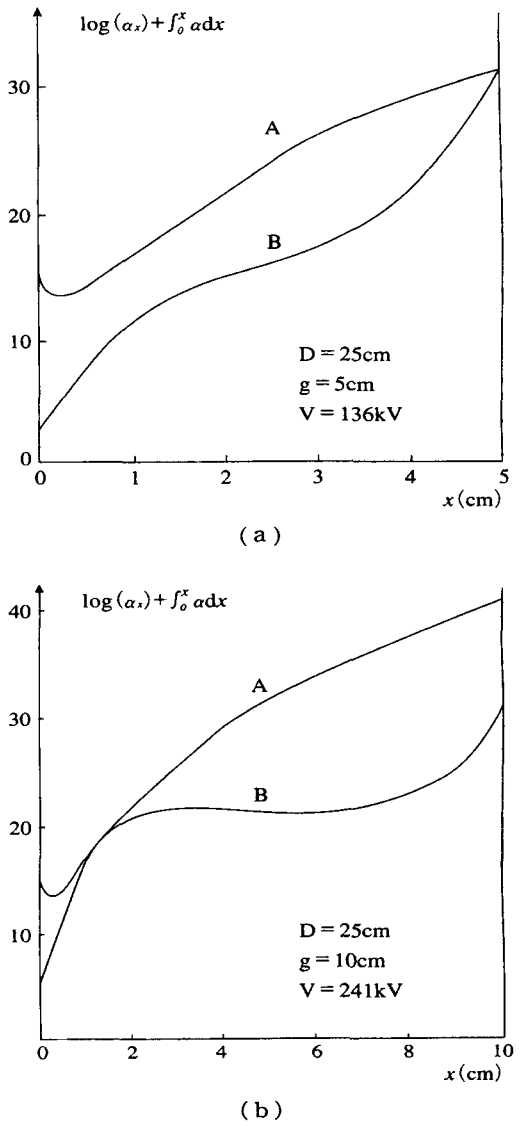

Fig. 7 Determination of sparkover voltage and critical avalanche length by Pedersen's method

Fig. 7 shows the application to the sphere diameter D of 25 cm, in which the ionization index **B** of a sphere gap is compared with the ionization index **A** of the parallel plane electrode.

The sparkover equation of the sphere gaps corresponding to **B** may be written as

$$\log_e(\alpha_x) + \int_0^x \alpha dx = g(x) \qquad (5)$$

where α_x is the numerical value of α at the avalanche head. In a uniform field where x is equal to gap length g and where α is constant, sparkover equation **A** becomes

$$g(x) = \log_e(\alpha) + \alpha x. \qquad (6)$$

The sparkover begins to occur when the value of g(x), found by solving (5), coincides with the value of g(x) in (6), and the calculated values of the voltage and position, respectively, denote the sparkover voltage and the critical avalanche length.

This method can be applied to any gap geometry of a well-known electric field distribution. The effect of the gap lengths on calculated sparkover voltages is shown in Fig. 7 (a) and (b), where the sphere diameter D is chosen as 25 cm.

Fig. 7 (a) shows the breakdown mechanism 1 for g=5 cm. Fig. 7 (b) shows the breakdown mechanism 2 for g=10 cm, which is nearly equal to the sphere radius r.

The sparkover voltage may change with the length and diameter of the shanks, in the range prescribed by IEC standard 60052.

Table 2 shows the results for the sphere diameters of 1.5 and 2 m, where the X class is for the smallest η, and the Y class is for the largest possible η.

Table 2 Calculation results of sparkover voltage affected by shank geometry, where **X** is for the min η and **Y** is for the max η. (Sphere diameters of 150 and 200 cm have negative polarity.)

D (cm)	150		200	
Class	**X**	**Y**	**X**	**Y**
g (cm)	V_s (kV)		V_s (kV)	
5	138	138		
10	265	265	265	265
30	754	754	758	758
50	1129	1141	1198	1204
70	1389	1419	1530	1548
90	1570	1619	1785	1820
100	1639	1699	1888	1933
110	1699	1769	1978	2033
130			2129	2203
150			2240	2334

4. Conclusions

From the field utilization factor η, calculated by the charge simulation method, the simple equation $\eta = 1-(g/3r)$ can be used as a representative value of the field utilization factor for standard sphere gaps. V_s is related to the maximum electric field E_m at sparkover as $E_m = V/(\eta g)$. E_m describes a U-curve for g/r, up to a diameter of 1 m. The curves of the maximum electric field for the 1.5-m and 2-m diameter are different from the U-form, because the standard values of the IEC standard have some irregularities at these points. For the 1.5-m and 2-m diameter, especially for negative polarity, the sparkover voltages have been calculated in the permitted range for the shank geometry of the IEC standard by integration of the ionization index.

References

[1] A. Pedersen, "Calculation of spark breakdown or corona voltages in nonuniform fields." *IEEE. Trans. PAS*, Vol.91, No.2, pp.200-206, 1967.

[2] F. H. Sanders, "Measurement of the Townsend coefficients for ionization by collision." *Phys. Rev.*, Vol.44, pp.1020-1024, 1933.

[3] Y. Nishikori, M. Murano and K. Kanaya, "Calculation of initial breakdown voltages of standard sphere gaps in air at atmospheric pressure by streamer criterion." Proc.8th. ISH. Yokohama, Vol.2, paper44.04, pp.101-104, 1993.

[4] Y. Nishikori, S. Kojima and T. Kouno, "A study of the field utilization factor and the maximum electric field at sparkover of the standard sphere gaps." *Electr. Eng. Jpn.*, Vol.139, No.4, pp.26-32, 2002.

[5] IEC 60052, 2002.10, Voltage measurement by means of standard air gaps.

[6] A. Schwaiger, "Beitrag zur elektrischen Festigkeitslehre." *Arch. Elektrotech.*, Vol.11, pp.41-50, 1922.

[7] M. Toepler, "Knickstelle im Verlauf der Anfangspannung." *Elektrotech. Z.*, Vol.51, pp.1219-1221, 1932.

[8] J. M. Meek, "A theoretical determination of breakdown voltage for sphere-gaps." *J. Franklin Inst.*, Vol.230, pp.229-242, 1940.

[9] F. W. Peek Jr., *Dielectric phenomenon in high voltage engineering*, McGraw-Hill, New York, 1915.

[10] T. Kawamoto and T. Takuma, "Influence of nearby objects and connecting leads on the electric field distribution of standard sphere gaps." *CRIEPI Report* 179003, 1979.

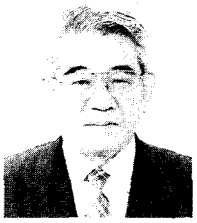

Yasuo Nishikori

He completed the master's course at Kogakuin University in 1968 and joined the Electrical Engineering Department there. After pursuing applied research on electron microscopes, he has been studying gas discharge, electric field computation, and high-voltage measurement technology since 1986. He is a lecturer of electrical engineering, and a member of the Japan Electron Microscope Society, the Applied Physics Society, and the Static Electricity Council.

Soji Kojima

He graduated from the Electrical Engineering Department at Tokyo University in 1963 and joined Toshiba Corporation. He was attached to the Lightning Arrester Center of the Hamakawasaki Factory. He has received the Denki Gakkai Progress Prize and Research Paper Award. He holds a Dr. Eng. Degree. After retiring in 1997, he became a professor at Kogakuin University, supervising electrical power systems engineering. He is pursuing research related to the Progress Prize and Research Paper Award. He is a member of IEEE.

Teruya Kouno

He completed his graduate studies at Tokyo University in 1962 and joined the Electrical Engineering Department there. After retiring in 1995, he became a professor at Kogakuin University, supervising high-voltage engineering. He has received the Research Paper Prize, Author Prize, and Electrical Power Prize from Denki Gakkai. He holds a Dr. Eng. Degree. He was the chairman of the Board of Editors at Denki Gakkai in 1980 and 1981. In1988 he was the head of the Tokyo branch of Denki Gakkai, and in 1991 supervised the A Division.